

PAPR Reduction of FBMC Signals Based on Uniform and Linear PDF Companding Schemes

Srinivas Ramavath · Umesh Chandra Samal

Received: date / Accepted: date

Abstract In this paper, two new companders are designed to reduce the ratio of peak to average power (PAPR) experienced by filter bank multicarrier (FBMC) signals. Specifically, the compander basic model is generalized, which alter the distributed FBMC signal amplitude peak. The proposed companders design approach provides better performance in terms of reducing the PAPR, Bit Error Rate (BER) and phase error degradation over the previously existing compander schemes. Many PAPR reduction approaches, such as the μ -law companding technique, are also available. It results in the formation of spectrum side lobes, although the proposed techniques result in a spectrum with fewer side lobes. The theoretical analysis of linear compander and expander transform for a few specific parameters are derived and analyzed. The suggested linear companding technique is analytically analysed using simulations to show that it efficiently decreases the high peaks in the FBMC system. **Keywords-** BER, CCDF, Compander, FBMC, OQAM, PAPR, PSD.

1 Introduction

The fifth generation (5G) network is to accommodate the envisioned Internet of Things (IoT) services, which requires high data rate ensuring reliability. One of the most challenging problems of upcoming wireless communication technology is a massive interconnection of users and devices for more flexibility and efficiency essential to support heterogeneous system requirements and to use spectrum efficiently as much as possible. To fulfill these requirements, new waveforms based on FBMC techniques have been proposed [1]. For future wireless communication systems, the FBMC with offset quadrature amplitude modulation is currently gaining a lot of attention [2, 3]. Using a prototype filter, FBMC-OQAM delivers great spectrum efficiency, enhanced time-frequency localisation, and very minimal out-of-band radiation [4]. However, in compared to OFDM signals, FBMC signals have a fundamentally different signal structure: adjacent signal data blocks overlap in FBMC systems,

Srinivas Ramavath
E-mail: srinivas2012iitg@gmail.com
School of Electronics Engineering, Kalinga Institute of Industrial Technology (KIIT) University

Umesh Chandra Samal
E-mail: umesh.samalfet@kiit.ac.in
School of Electronics Engineering, Kalinga Institute of Industrial Technology (KIIT) University

whereas symbols in OFDM systems do not [5,6]. Therefore, the PAPR of FBMC systems is quite different from OFDM systems and needs to be reduced for the better performance [7].

Signal distortion happens when big peaks enter a nonlinear section of a high-power amplifier (HPA) without being preprocessed [8]. As a result, reducing the signal peak power is a good way to alleviate the high PAPR problem. So for In the literature, many PAPR reduction techniques have been devised [9, 10]. There are three primary categories in which these schemes may be classified: Techniques for signal distortion, signal scrambling, and coding. Before passing through the HPA, signal distortion methods lower the PAPR of FBMC signals. Filtering and clipping [6], peak windowing, peak cancellation, and other companding techniques [11–13] are among the most well-known signal distortion techniques. These approaches considerably reduce the power ratio, but they also create in-band and out-of-band distortion [14], resulting in BER degradation. The alternative option is to rearrange the data symbols without altering the way signals are generated. such as the selective mapping (SLM) [15–17], tone reservation (TR) [18], partial transmission sequence (PTS) [19–21] and active constellation extension (ACE) [22–25]. It should be emphasised that the two categories listed above are rarely antagonistic. Modifying and extending the PAPR reduction methods for FBMC signals to Companded FBMC signals is a natural way [26].

The FBMC system is explored in this study [27–29], which includes two unique companding operations at the transmitter. The authentic signal amplitude is changed into a predetermined distribution in this work to reallocate the statistics of the compounded signal more freely. The uniform and nonlinear companding techniques are presented in particular to deal with signal distortion. The theoretical and simulation result show that the proposed techniques suppresses the PAPR more effectively. The nonlinear companding technique achieves a better bit error rate (BER) than other companding techniques.

The rest of this paper is laid out as follows. The FBMC system model and problem description are described in Section II. In section III, we derive a theoretical analysis of the proposed schemes. In section IV, the PAPR and BER performance are simulated and compared with the previously existing μ -law companding scheme. Finally, it is conclude in Section V.

2 FBMC SYSTEM Model

2.1 Transmitted Signal

In FBMC system, the input m^{th} complex data symbol for k^{th} subcarrier can represented as

$$x_k(m) = a_k(m) + jb_k(m), \quad 0 \leq k \leq K-1, \quad 0 \leq m \leq M-1 \quad (1)$$

The real and imaginary components of the m^{th} symbol for the k^{th} subcarrier are $a_k(m)$ and $b_k(m)$, respectively. For every K sub-carriers, the m^{th} symbols input data block $x(m)$ is provided by

$$x(m) = [x_0(m), x_1(m), \dots, x_{K-1}(m)]^T \quad (2)$$

In the time domain, the real and imaginary components of each symbol are tagged by $\frac{T}{2}$, which is half of the data block period (T). The data blocks are modulated using K distinct sub-carrier modulators, whose carrier frequencies are spaced by the inverse of the symbol

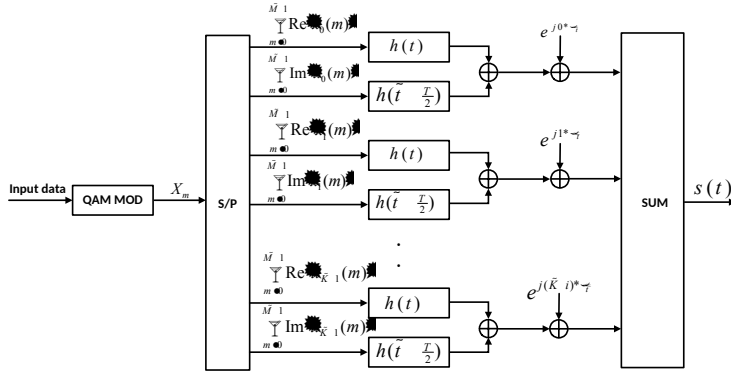


Fig. 1: The FBMC-OQAM system transmitter

period ($\frac{1}{T}$). The M data block modulated signal generated by the OQAM-FBMC is represented as

$$S(t) = \sum_{k=0}^{K-1} \sum_{m=0}^{M-1} S_m^k(t) \quad (3)$$

The FBMC system k^{th} sub-carrier and m^{th} symbol signal is expressed as

$$S_m^k(t) = \left[\text{Re}(x_k) h(t - mT) + \text{Im}(x_k) h(t - mT - \frac{T}{2}) \right] e^{jk\phi_t} \quad (4)$$

where $\phi_t = \frac{2\pi}{T}t + \frac{\pi}{2}$, $0 \leq t \leq (M + \alpha - \frac{1}{2})T$ and the time domain impulse response with finite length αT is denoted by $h(t)$. Because the prototype filter response in FBMC-OQAM systems has a longer time period than T , surrounding data signal blocks overlap.

2.2 Problem Description

Each symbol in an OFDM system has a length of N and a rate of $\frac{1}{N}$. A set of N orthogonal sub-carriers modulates the OFDM input data complex symbol $X(k)$ for $0 \leq k \leq N-1$, For $0 \leq n \leq N-1$, the output $x(n)$ is represented as

$$x(n) = \frac{1}{N} \sum_{k=0}^{N-1} X(k) e^{j\frac{2\pi}{N}nk}, \quad 0 \leq n \leq N-1 \quad (5)$$

There are no overlaps between neighbouring OFDM symbols, and the power ratio of the OFDM system is calculated per symbol [5].

$$PAPR_{OFDM} = \frac{1}{P_{avg}} \max_{0 \leq n \leq N-1} |x(n)|^2 \quad (6)$$

The FBMC-OQAM signals in the time domain are overlapping with signals from the OFDM system that have been changed. The FBMC modulated signal $s(t)$ can be broken into symbols of length T over which the PAPR can be calculated for precise peak to average power ratio comparisons to 4G systems. The procedure of measuring the PAPR over two symbols

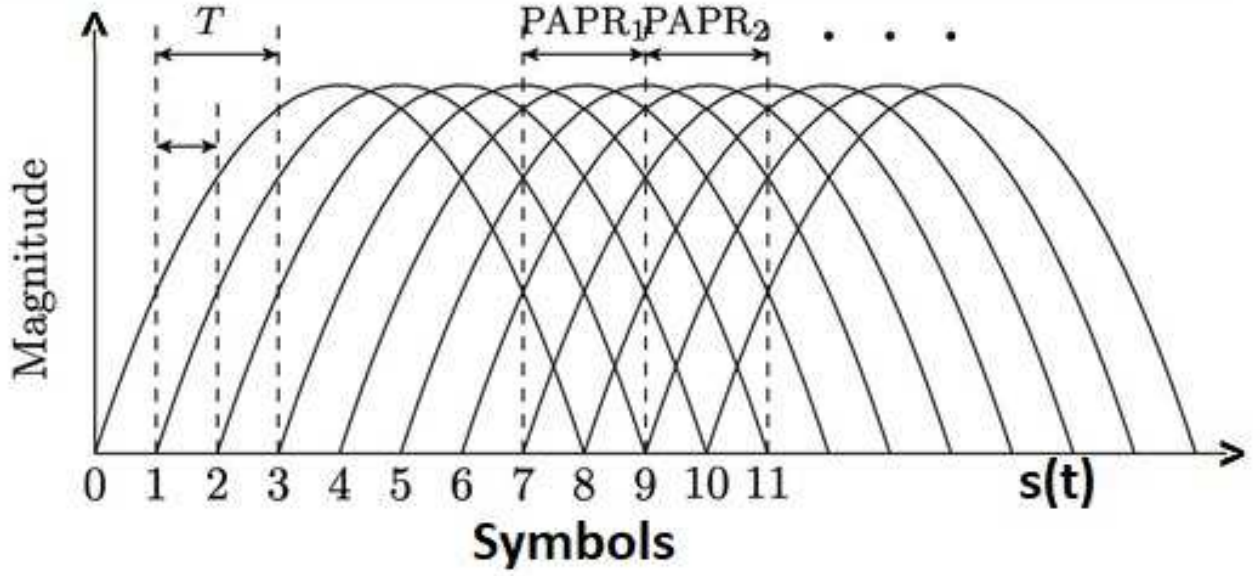


Fig. 2: FBMC Overlapping symbols

of length T , each shown by $PAPR_1$ and $PAPR_2$, is depicted in Fig. 2. We can define the PAPR over length T in a frame based on that concept [25].

Each part of $S(t)$ has length T because it is initially split into $M + \alpha$ parts. The power ratio for $S(t)$ in the i^{th} interval is then calculated as [1]

$$PAPR_{FBMC} = \frac{1}{P_{avg}} \max_{iT \leq t \leq (i+1)T} |S(t)|^2 \quad (7)$$

where $i = 0, 1, 2, \dots, M + \alpha - 1$. To simplify Eq.(4), denote $X_k(m) = Re(x_k)$ if m is even, and $X_k(m) = Im(x_k)$ if m is odd. Then, Eq. (4) can be rewritten as

$$S(t) = \sum_{k=0}^{K-1} \sum_{m=0}^{M-1} X_k(m) h(t - \frac{mT}{2}) e^{j(\frac{2\pi}{T}t + \phi_m^k)} \quad (8)$$

where $\phi_m^k = \frac{\pi}{2}(m+k) - \pi mk$ hence, the k^{th} subcarrier signals can be expressed as

$$S^k(t) = \sum_{m=0}^{M-1} X_k(m) h(t - \frac{mT}{2}) e^{j(\frac{2\pi}{T}kt + \phi_m^k)} \quad (9)$$

The FBMC system transmitted signal is given as

$$S(t) = \sum_{k=0}^{K-1} S^k(t) \quad (10)$$

The variance is σ_x^2 , and $X_k(m)$ is a statistically identical independent distribution (i.i.d.). The mean and variance of $S^k(t)$ is 0 and $\sigma_k^2 = \sigma_x^2 \sum_{m=0}^{M-1} h(t - \frac{mT}{2})^2$ respectively. $S^k(t)$ has a mean

of 0 and a variance of $\sigma_k^2 = \sigma_x^2 \sum_{m=0}^{M-1} h\left(t - \frac{mT}{2}\right)^2$, respectively. $E[S^k(t)]$ is uncorrelated with σ_k^2 and k . The $s(t)$ real and imaginary components approach Gaussian distribution with zero mean and variance $\sigma_s^2 = k \frac{\sigma_x^2}{2}$ when k is considered as large as possible by the central limit theorem.

The $s(t)$ absolute square ($|S(t)|^2$) follows a central chi-squared distribution, probability density function (pdf) of $|S(t)|^2$ define as

$$P_Y(y) = \frac{1}{2\sigma_s^2} e^{-\frac{y}{2\sigma_s^2}} \quad (11)$$

Then, supposing

$$Z = \frac{|S(t)|^2}{E[|S(t)|^2]} \quad (12)$$

Finally probability density function of Z written as

$$\begin{aligned} P_Z(z) &= 2\sigma_x^2 P_Y(2\sigma_x^2 z) \\ &= \alpha_t e^{-\alpha_t z} \end{aligned} \quad (13)$$

where $\alpha_t = \frac{2}{k \sum_{m=0}^{M-1} h\left(t - \frac{mT}{2}\right)^2}$. The cumulative distribution function (CDF) for Z can be written as follows:

$$\begin{aligned} P(z \leq \gamma) &= \int_0^\gamma P_Z(z) dz \\ &= \int_0^\gamma \alpha_t e^{-\alpha_t z} dz \\ &= 1 - e^{-\alpha_t \gamma} \end{aligned} \quad (14)$$

As a result, the PAPR distribution function for FBMC can be expressed as

$$\begin{aligned} P(\text{PAPR} \leq \gamma) &= P\left(\bigcap_{i=nT}^{(n+1)T-1} |S_0(t)|^2 \leq \gamma\right) \\ &= \prod_{i=nT}^{(n+1)T-1} P(|S_0(t)|^2 \leq \gamma) \\ &= \prod_{i=nT}^{(n+1)T-1} (1 - e^{-\alpha_t \gamma}) \end{aligned} \quad (15)$$

How PAPR is critical for FBMC system and its requirement, which may cause a severe non-linear distortion by the power amplifier (PA). Therefore, it is necessary to design an effective technique to mitigate the distortion. With an appropriate choice of the companding function can be reduce more peak power. The proposed method is expected to achieve acceptable PAPR.

3 Proposed Schemes

A unique peice-wise linear function scheme that can effectively improve the PAPR reduction and the BER performance of FBMC transmitted signals is proposed. The nonlinear companding [30] transform is given by $y_n = h(x_n)$, here x_n is the FBMC original signal and the nonlinear companded output signal is y_n , the peice-wise linear function $h(\cdot)$ only changes the input signals amplitudes.

3.1 Companding Based on nonlinear function

Assume the transform $y_1 = h_1(x_n)$ and the pdf of y_1 , the inflection point and the cutoff point are $c\sigma$ and A_c respectively depicts in fig. 3.

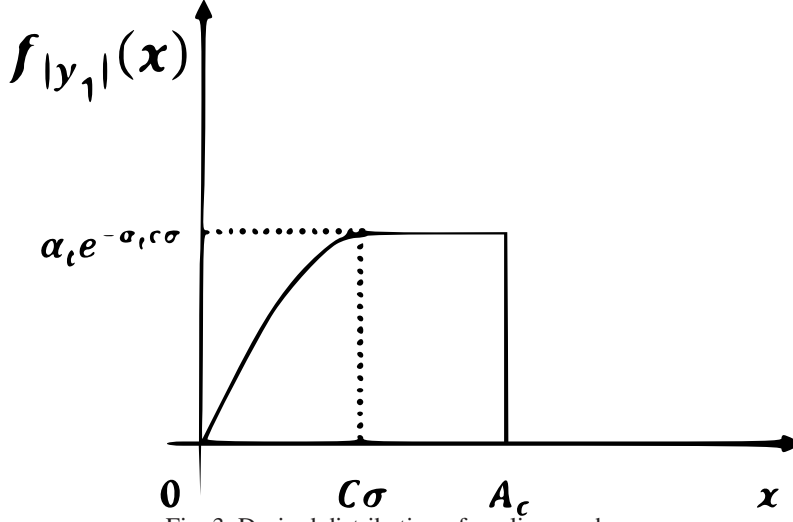


Fig. 3: Desired distribution of nonlinear scheme

The pdf of $|y_1|$ is same as pdf of $|x_n|$ between $[0, c\sigma]$; In the interval $[c\sigma, A_c]$, the pdf of $|y_1|$ has a uniformly distributed. The inflection and cutoff point coordinates are $(c\sigma, f_{|x_n|}(x))$ and $(A_c, f_{|x_n|}(x))$, respectively. Therefore, the $|y_1|$ pdf can be represented as

$$f_{|y_1|}(x) = \begin{cases} \frac{2x}{\sigma^2} e^{-\frac{x^2}{\sigma^2}} & 0 \leq x \leq c\sigma \\ f_{|x_n|}(c\sigma) & c\sigma \leq x \leq A_c \end{cases} \quad (16)$$

The area of the probability density function (pdf) $\int_0^\infty f_{|y_1|}(x) dx = 1$, we can obtain $A = (c + \frac{1}{2c})\sigma$. The pdf of $|y_1(t)|^2$ define as

$$f_{|y_1(t)|^2}(x) = \begin{cases} \frac{1}{2\sigma^2} e^{-\frac{x}{2\sigma^2}} & 0 \leq x \leq c\sigma \\ \frac{2c}{\sigma} e^{-c^2} & c\sigma \leq x \leq A_c \end{cases} \quad (17)$$

Then, supposing

$$Z_1 = \frac{|y_1(t)|^2}{E[|y_1(t)|^2]} \quad (18)$$

Finally probability density function of Z_1 written as

$$f_{z_1}(z) = \begin{cases} \alpha_t e^{-\alpha_t z} & 0 \leq z \leq c\sigma \\ \beta_t & c\sigma \leq z \leq A_c \end{cases} \quad (19)$$

Where $\beta_t = 4\alpha_t c\sigma e^{-c^2}$. The cumulative distribution function (CDF) for Z_1 can be expressed as

$$F_{z_1}(z) = \begin{cases} 1 - e^{-\alpha_t z} & 0 \leq z \leq c\sigma \\ \beta_t z & c\sigma \leq z \leq A_c \end{cases} \quad (20)$$

Hence, the PAPR distribution function for FBMC can be expressed as

$$\begin{aligned}
 P(\text{PAPR} \leq \gamma) &= P\left(\bigcap_{i=nT}^{(n+1)T-1} |S_0(t)|^2 \leq \gamma\right) \\
 &= \prod_{i=nT}^{(n+1)T-1} P(|S_0(t)|^2 \leq \gamma) \\
 &= \prod_{i=nT}^{(n+1)T-1} \begin{cases} 1 - e^{-\alpha_t z} & 0 \leq x \leq c\sigma \\ \beta_t z & c\sigma \leq x \leq A_c \end{cases}
 \end{aligned} \tag{21}$$

Considering the input signal phase, the monotonic increasing function $h_1(x)$ is represented as

$$h_1(x) = \text{sgn}(x) F_{|y_1|}^{-1}(F_{|x_n|}(x)) \tag{22}$$

here $\text{sgn}(x)$ indicates the signum function. Thus, the nonlinear companding function at the transmitter can be obtained as

$$h_1(x) = \begin{cases} x & |x| \leq c\sigma \\ \text{sgn}(x) \frac{\sigma}{c} \left(\frac{2}{3} - \frac{1}{2} e^{\frac{1}{c^2} - \frac{x^2}{\sigma^2}} \right) & |x| > c\sigma \end{cases} \tag{23}$$

At the receiver is the reciprocal of companding transform is

$$h_1^{-1}(x) = \begin{cases} x & |x| \leq c\sigma \\ \text{sgn}(x) \frac{\sigma}{c^2} \sqrt{\frac{1}{c^2} - \frac{1}{c^4} \ln\left(\frac{4c\sigma - x}{3c\sigma}\right)} & |x| > c\sigma \end{cases} \tag{24}$$

3.2 Companding Based on linear function

Assume the transform $y_2 = h_2(x_n)$ and the y_2 pdf, the inflection point and the cutoff point are $c\sigma$ and A_c respectively depicts in fig. 4.

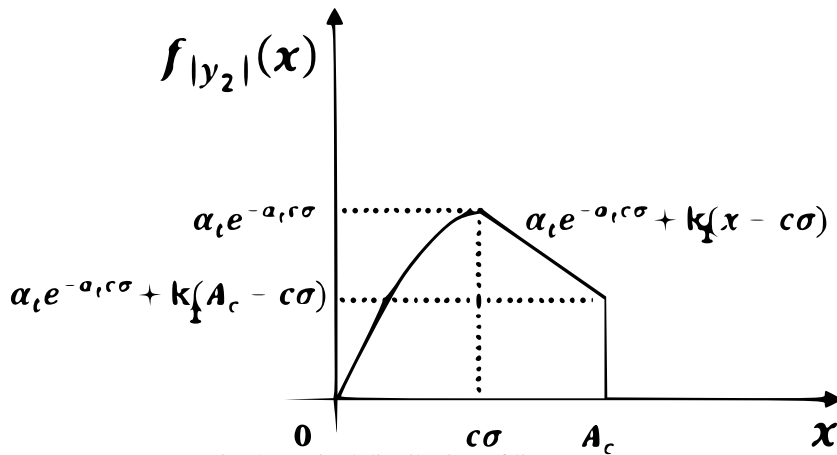


Fig. 4: Desired distribution of linear scheme

The pdf of $|y_2|$ is identical with $|x_n|$ between $[0, c\sigma]$; In the interval $[c\sigma, A_c]$, the pdf of $|y_2|$ has linear function with a slope k_1 distributed. The inflection and cutoff point coordinates are $(c\sigma, f_{|x_n|}(x))$ and $(A_c, f_{|x_n|}(x))$, respectively. Therefore, the $|y_2|$ pdf can be expressed as

$$f_{|y_2|}(x) = \begin{cases} \frac{2x}{\sigma^2} e^{-\frac{x^2}{\sigma^2}} & 0 \leq x \leq c\sigma \\ k_1 x + \alpha_t e^{-\delta_t} - k_1 c\sigma & c\sigma \leq x \leq A_c \end{cases} \quad (25)$$

From the definition of CDF $F_{|y_2|}(A_c) = 1$, we have obtain $k_1 = \frac{4\sigma c^2 - 2A_c C + \sigma}{\sigma A_c - c\sigma^2} e^{-c^2}$. The probability density function (pdf) of $|y_2(t)|^2$ define as

$$f_{|y_2(t)|^2}(x) = \begin{cases} \frac{1}{2\sigma^2} e^{-\frac{x}{2\sigma^2}} & 0 \leq x \leq c\sigma \\ \frac{ce^{-c^2}}{\sigma\sqrt{y}} + \frac{k_1}{2} \left(1 - \frac{c\sigma}{\sqrt{y}}\right) & c\sigma \leq x \leq A_c \end{cases} \quad (26)$$

Then, supposing

$$Z_2 = \frac{|y_2(t)|^2}{E[|y_2(t)|^2]} \quad (27)$$

Finally probability density function of Z_2 written as

$$f_{Z_2}(z) = \begin{cases} \alpha_t e^{-\alpha_t z} & 0 \leq z \leq c\sigma \\ \frac{ce^{-c^2}}{\sigma} \sqrt{\frac{2\sigma_x}{z}} + k_1 \sigma_x \left(1 - \frac{c\sigma}{\sqrt{2\sigma_x z}}\right) & c\sigma \leq z \leq A_c \end{cases} \quad (28)$$

The Z_2 cumulative distribution function (CDF) can be written as

$$F_{Z_2}(z) = \begin{cases} 1 - e^{-\alpha_t z} & 0 \leq z \leq c\sigma \\ \frac{2ce^{-c^2}}{\sigma} \sqrt{2\sigma_x z} + k_1 \sigma_x \left(z - 2c\sigma \sqrt{\frac{z}{\sigma_x}}\right) & c\sigma \leq z \leq A_c \end{cases} \quad (29)$$

Hence, for FBMC, the PAPR distribution function can be expressed as

$$\begin{aligned} P(\text{PAPR} \leq \gamma) &= P\left(\bigcap_{i=nT}^{(n+1)T-1} |S_0(t)|^2 \leq \gamma\right) \\ &= \prod_{i=nT}^{(n+1)T-1} P\left(|S_0(t)|^2 \leq \gamma\right) \\ &= \prod_{i=nT}^{(n+1)T-1} \begin{cases} 1 - e^{-\alpha_t z} & 0 \leq z \leq c\sigma \\ \frac{2ce^{-c^2}}{\sigma} \sqrt{2\sigma_x z} + k_1 \sigma_x \left(z - 2c\sigma \sqrt{\frac{z}{\sigma_x}}\right) & c\sigma \leq z \leq A_c \end{cases} \end{aligned} \quad (30)$$

Considering the input signal phase, the monotonic increasing function $h_2(x)$ is represented as

$$h_2(x) = \text{sgn}(x) F_{|y_1|}^{-1}(F_{|x_n|}(x)) \quad (31)$$

here $\text{sgn}(x)$ indicates the signum function. Thus, the nonlinear companding function at the transmitter can be obtained as

$$h_2(x) = \begin{cases} x & |x| \leq c\sigma \\ \text{sgn}(x) \frac{1}{k_1} \left(k_1 c\sigma - \frac{2c}{\sigma} e^{-c^2} + \sqrt{\frac{4c^2}{\sigma^2} e^{-2c^2} + 2k_1 \left(e^{-c^2} - e^{-\frac{x^2}{\sigma^2}} \right)} \right) & |x| > c\sigma \end{cases} \quad (32)$$

At the receiver is the reciprocal of companding transform is

$$h_2^{-1}(x) = \begin{cases} x & |x| \leq c\sigma \\ \text{sgn}(x) \sqrt{-\sigma^2 \ln \left(-\frac{k}{2}x^2 + c \left(k_1\sigma - \frac{2}{\sigma e^{-c^2}} \right) x - \frac{k_1 c^2 \sigma^2}{2} + e^{-2c^4 - c^2} \right)} & |x| > c\sigma \end{cases} \quad (33)$$

3.3 Theoretical Analysis

The Bussgang theorem extension can be used to express real or complex Gaussian signals as the sum of an appropriate compressed input replica and an uncorrelated nonlinear signal distortion noise [31]. Hence, the reconstructed signal y_n can be formed as

$$y_n = \alpha x_n + u_n \quad (34)$$

here the FBMC signal x_n is not stationary because of α is attenuation factor [32] and the FBMC signal promises α to be time invariant given as $\alpha = \frac{E\{y_n x_n^*\}}{E\{x_n x_n^*\}}$ and assume a constant average power level throughout the companding process expressed as

$$\begin{aligned} P_{y_n} &= P_{\alpha x_n} + P_{u_n} \\ &= \alpha^2 P_{x_n} + P_{u_n} \Rightarrow P_{u_n} \\ &= (1 - \alpha^2) P_{x_n} \end{aligned} \quad (35)$$

Where, $0 < \alpha < 1$. For $\alpha \rightarrow 1$, the smaller P_{u_n} will be the reconstructed signal x'_n at the receiver. Which is given by $x'_n = \beta y_n + z_n$, where $\beta = \frac{1}{\alpha}$, $z_n = \frac{u_n}{\alpha}$. Due to homogeneity, the received signal expressed as $r_n = y_n + w_n$, where w_n is the Gaussian channel noise. A transform gain G is defined as the ratio of the original signal's PAPR to the combined signal's PAPR.

$$G_y \text{dB} = 10 \cdot \log_{10} \frac{\text{PAPR}_x}{\text{PAPR}_y} \quad (36)$$

4 SIMULATIONS ANALYSIS

In this section, simulations are used to evaluate the proposed techniques. Consider 10,000 symbols with 512 sub-carriers for the suggested linear scheme signal transmission. The PHYDYAS prototype filter with an overlapping factor of 4 is then applied to the symbols $x_k(m)$ [4]. Fig. 5 shows how different methods perform in terms of PAPR reduction. The CCDF at 10^{-2} , the PAPR 4dB, which is 1.1dB and 6.3dB smaller than that of the μ law companding and original signals respectively. A greater reduction can be achieved by proposed linear scheme, which results in 10 dB enhances then the conventional scheme.

Fig. 5 depicts CCDF curves of various FBMC systems with different length of subcarriers 512 and 1024. When number of subcarriers increasing the PAPR also increasing but in proposed nonlinear scheme is less effected compared with other exiting schemes. Depicts in Table I, to gain a PAPR of 1.0dB the maximum number subcarriers required is 1024. The required PAPRs under the conventional, μ -law, uniform and nonlinear companding schemes are 10.6dB, 5.4dB, 4.9dB and 1.2dB respectively.

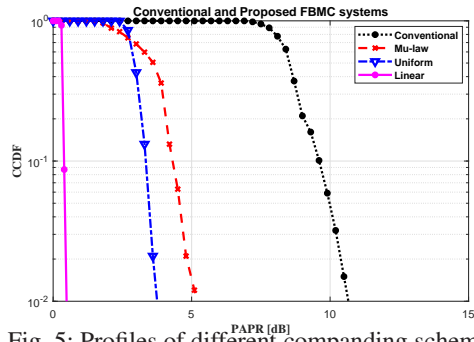


Fig. 5: Profiles of different companding schemes

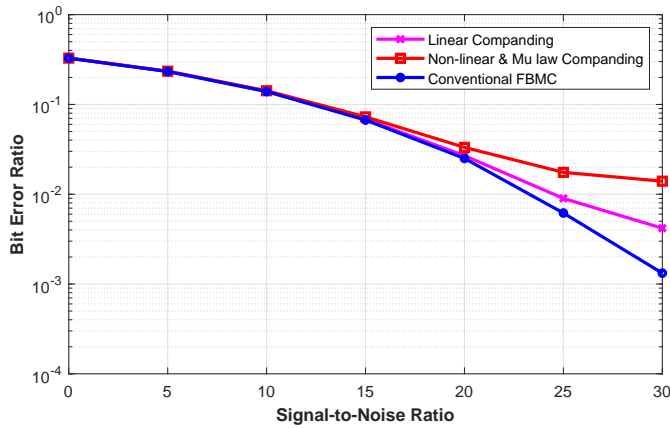


Fig. 6: BER of different companding schemes

Fig. 6 illustrates the BER performance of the conventional and different designed non-linear FBMC schemes, the AWGN channel is assumed in the simulations. Specially, in Table I, to attain a BER of 10^{-3} , the minimum signal to noise ratio (E_g/N_0) required is 30dB. The required E_g/N_0 under the conventional, μ -law, uniform and linear companding schemes are 30dB, 40dB, 40dB and 33dB, respectively.

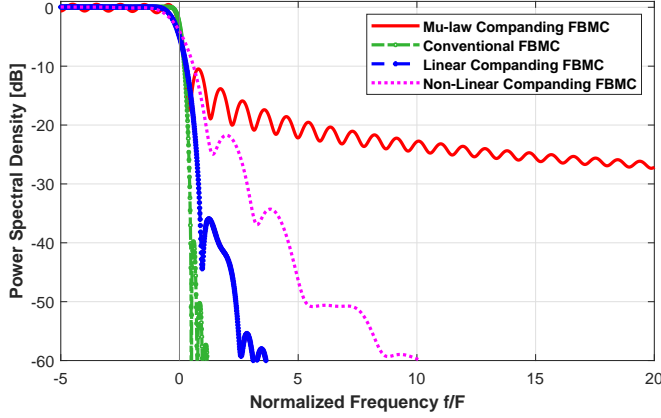


Fig. 7: PSD of different companding schemes

Fig. 7 illustrates the PSD simulation performance of the conventional and different designed nonlinear FBMC schemes. Specially, in Table I, the required PSD under the conventional, μ -law, uniform and linear companding schemes are -40dB, -10dB, -22dB and -37dB, respectively.

FBMC Systems	SNR (dB)		PAPR (dB)		PSD(dB)
	BER= 10^{-2}	BER= 10^{-3}	K=512	K=1024	
Conventional	23	30	10.3	10.6	-40
μ -law	35	40	5.1	5.4	-10
Uniform	35	40	4.0	4.9	-22
Linear	25	33	1.0	1.2	-37

Table 1: PAPR, BER and PSD with different companding

5 CONCLUSIONS

In this paper, the theoretical PAPR expression of an efficient companding FBMC schemes are derived. Through a specially designed nonlinear companding process, the innovative technology maintains a steady average power level. Hence, the efficiency of the HPA can be improved. The proposed nonlinear scheme may meet various scheme criteria by reducing the effective power ratio and improving the BER performance. The proposed schemes are numerous particular examples of the basic μ -law companding, piecewise, and Tangent companding techniques. Additionally, it has been proven through a theoretical analysis that the developed scheme can reduce distortion better than existing schemes. It is further proven that when the slope k_1 is modest enough, the de-companding operation at the receiver side is no longer required. The designed linear companding technique might outperform the μ -law companding scheme in terms of power ratio reduction, PSD and BER performance, according to simulation findings.

References

1. Umesh Chandra Samal, Bhargav Appasani, and Dusmanta Kumar Mohanta. 5g communication networks and modulation schemes for next-generation smart grids. In *Smart Grids and Their Communication Systems*, pages 361–399. Springer, 2019.
2. Tao Jiang, Da Chen, Chunxing Ni, and Daiming Qu. *OQAM/FBMC for future wireless communications: Principles, technologies and applications*. Academic Press, 2017.
3. Ronald Nissel, Stefan Schwarz, and Markus Rupp. Filter bank multicarrier modulation schemes for future mobile communications. *IEEE Journal on Selected Areas in Communications*, 35(8):1768–1782, 2017.
4. Maurice Bellanger, D Le Ruyet, D Roviras, M Terré, J Nossek, L Baltar, Q Bai, D Waldhauser, M Renfors, T Ihalainen, et al. Fbmc physical layer: a primer. *PHYDYAS, January*, 25(4):7–10, 2010.
5. Ramjee Prasad. *OFDM for wireless communications systems*. Artech House, 2004.
6. Yong Soo Cho, Jaekwon Kim, Won Y Yang, and Chung G Kang. *MIMO-OFDM wireless communications with MATLAB*. John Wiley & Sons, 2010.
7. Srinivas Ramavath and Rakesh Singh Kshetrimayum. Analytical calculations of ccdf for some common papr reduction techniques in ofdm systems. In *2012 International Conference on Communications, Devices and Intelligent Systems (CODIS)*, pages 393–396. IEEE, 2012.
8. Changyoung An and Heung-Gyoon Ryu. Design and performance comparison of w-ofdm under the nonlinear hpa environment. *Wireless Personal Communications*, 98(1):983–999, 2018.
9. Zongmiao He, Lingyu Zhou, Yiou Chen, and Xiang Ling. Filter optimization of out-of-band emission and ber analysis for fbmc-oqam system in 5g. In *2017 IEEE 9th International Conference on Communication Software and Networks (ICCSN)*, pages 56–60. IEEE, 2017.
10. Dongjun Na and Kwonhue Choi. Low papr fbmc. *IEEE Transactions on Wireless Communications*, 17(1):182–193, 2017.
11. Lei Zhang, Ayesha Ijaz, Pei Xiao, Mehdi M Molu, and Rahim Tafazolli. Filtered ofdm systems, algorithms, and performance analysis for 5g and beyond. *IEEE Transactions on Communications*, 66(3):1205–1218, 2017.
12. Bamidele Adebisi, Kelvin Anoh, and Khaled M Rabie. Enhanced nonlinear companding scheme for reducing papr of ofdm systems. *IEEE Systems journal*, 13(1):65–75, 2018.
13. Tao Jiang, Weidong Xiang, Paul C Richardson, Daiming Qu, and Guangxi Zhu. On the nonlinear companding transform for reduction in papr of mcm signals. *IEEE Transactions on Wireless Communications*, 6(6):2017–2021, 2007.
14. Rostom Zakaria and Didier Le Ruyet. Theoretical analysis of the power spectral density for fft-fbmc signals. *IEEE Communications Letters*, 20(9):1748–1751, 2016.
15. SS Krishna Chaitanya Bulusu, Hmaied Shaiek, Daniel Roviras, and Rafik Zayani. Reduction of papr for fbmc-oqam systems using dispersive slm technique. In *2014 11th International Symposium on Wireless Communications Systems (ISWCS)*, pages 568–572. IEEE, 2014.
16. Jinwei Ji, Guangliang Ren, and Huining Zhang. A semi-blind slm scheme for papr reduction in ofdm systems with low-complexity transceiver. *IEEE Transactions on Vehicular Technology*, 64(6):2698–2703, 2014.
17. Li Li, Daiming Qu, and Tao Jiang. Partition optimization in ldpc-coded ofdm systems with pts papr reduction. *IEEE Transactions on Vehicular Technology*, 63(8):4108–4113, 2014.
18. Shixian Lu, Daiming Qu, and Yejun He. Sliding window tone reservation technique for the peak-to-average power ratio reduction of fbmc-oqam signals. *IEEE Wireless Communications Letters*, 1(4):268–271, 2012.
19. Kang-Seok Lee, Young-Jeon Cho, Jun-Young Woo, Jong-Seon No, and Dong-Joon Shin. Low-complexity pts schemes using ofdm signal rotation and pre-exclusion of phase rotating vectors. *Iet Communications*, 10(5):540–547, 2016.
20. Honggui Deng, Shuang Ren, Yan Liu, and Chengying Tang. Modified pts-based papr reduction for fbmc-oqam systems. In *Journal of Physics: Conference Series*, volume 910, page 012057. IOP Publishing, 2017.
21. Chen Ye, Zijun Li, Tao Jiang, Chunxing Ni, and Qi Qi. Papr reduction of oqam-ofdm signals using segmental pts scheme with low complexity. *IEEE Transactions on Broadcasting*, 60(1):141–147, 2013.
22. Nuan Van der Neut, Bodhaswar TJ Maharaj, Frederick De Lange, Gustavo J González, Fernando Gregorio, and Juan Cousseau. Papr reduction in fbmc using an ace-based linear programming optimization. *EURASIP Journal on Advances in Signal Processing*, 2014(1):1–21, 2014.
23. Zhixing Yang, Haidong Fang, and Changyong Pan. Ace with frame interleaving scheme to reduce peak-to-average power ratio in ofdm systems. *IEEE Transactions on Broadcasting*, 51(4):571–575, 2005.
24. Zilong Liu, Pei Xiao, and Su Hu. Low-papr preamble design for fbmc systems. *IEEE Transactions on Vehicular Technology*, 68(8):7869–7876, 2019.

25. Fangyu Cui, Yunlong Cai, Minjian Zhao, Ming Lei, and Lajos Hanzo. Peak-to-average power ratio reduction based on penalty-cccp for filter bank multicarrier systems. *IEEE Transactions on Vehicular Technology*, 68(11):11353–11357, 2019.
26. Srinivas Ramavath and Umesh Chandra Samal. Theoretical analysis of papr companding techniques for fbmc systems. *Wireless Personal Communications*, 118(4):2965–2981, 2021.
27. Job Chunkath and VS Sheeba. Constrained message length coding for low peak to average power ratio in fbmc: Oqam systems. *Wireless Personal Communications*, 116(4):2981–2996, 2021.
28. MN Geetha and UB Mahadevaswamy. Performance evaluation and analysis of peak to average power reduction in ofdm signal. *Wireless Personal Communications*, 112(4):2071–2089, 2020.
29. Mohit Kumar Srivastava, Manoj Kumar Shukla, Neelam Srivastava, and Ashok Kumar Shankhwar. A hybrid scheme for low papr in filter bank multi carrier modulation. *Wireless Personal Communications*, 113(2):1009–1028, 2020.
30. Shri Ramtej Kondamuri and Anuradha Sundru. Non linear companding transform to mitigate papr in dct based sc-fdma system. *Wireless Personal Communications*, pages 1–20, 2020.
31. Davide Dardari, Velio Tralli, and Alessandro Vaccari. A theoretical characterization of nonlinear distortion effects in ofdm systems. *IEEE transactions on Communications*, 48(10):1755–1764, 2000.
32. Paolo Banelli. Theoretical analysis and performance of ofdm signals in nonlinear fading channels. *IEEE Transactions on Wireless Communications*, 2(2):284–293, 2003.

